Relationship Between Visual Acuity and Retinal Structures Measured by Spectral Domain Optical Coherence Tomography in Patients With Open-Angle Glaucoma

Ji Hyun Kim,[1] Hye Sun Lee,[2] Na Rae Kim,[3] Gong Je Seong,[4] and Chan Yun Kim[4]

[1]Siloam Eye Hospital, Seoul, Korea
[2]Department of Research Affairs, Yonsei University College of Medicine, Seoul, Korea
[3]Department of Ophthalmology, Inha University School of Medicine, Incheon, Korea
[4]Institute of Vision Research, Department of Ophthalmology, Yonsei University College of Medicine, Seoul, Korea

Correspondence: Chan Yun Kim, Institute of Vision Research, Department of Ophthalmology, Yonsei University College of Medicine, 134 Shinchon-dong, Seodaemun-gu, Seoul, Korea 120-752; kcyeye@yuhs.ac.

Submitted: August 13, 2013
Accepted: July 3, 2014

Citation: Kim JH, Lee HS, Kim NR, Seong GJ, Kim CY. Relationship between visual acuity and retinal structures measured by spectral domain optical coherence tomography in patients with open-angle glaucomaa. *Invest Ophthalmol Vis Sci*. 2014;55:4801–4810. DOI:10.1167/iovs.13-13052

Purpose. We assessed the relationship between retinal structures measured by spectral-domain optical coherence tomography (SD-OCT) and visual acuity in open-angle glaucoma (OAG) patients.

Methods. In this cross-sectional observational study, 186 eyes from 186 OAG patients were included. The participants underwent RTVue OCT for measurement of circumpapillary retinal nerve fiber layer (cpRNFL) thickness and macular ganglion cell complex (mGCC) thickness. The correlations between best-corrected visual acuity (BCVA) and optical coherence tomography (OCT) parameters were evaluated using Pearson's partial correlation test and regression analysis. Receiver operating characteristic (ROC) curve analysis was performed to obtain a cutoff value for OCT parameters in detecting decreased visual acuity (BCVA < 0.7).

Results. Among RNFL parameters, average RNFL thickness ($r = -0.447$, $P < 0.001$) showed the highest correlation with BCVA, followed by superior hemisphere ($r = -0.440$, $P < 0.001$), and TU1 (67.5°–90°, $r = -0.427$, $P < 0.001$), TU2 (45°–67.5°, $r = -0.408$, $P < 0.001$), and TL1 (90°–112.5°, $r = -0.40$, $P < 0.001$) sectors. When logMAR BCVA was plotted against average RNFL/ganglion cell complex (GCC) thickness, second-order polynomial models fit better than the linear model. The areas under the receiver operating characteristic curves (AUROCs) of the average RNFL/GCC thickness were 0.910 (95% confidence interval [CI], 0.856–0.965) and 0.874 (95% CI, 0.795–0.953), respectively.

Conclusions. The relationship between BCVA and SD-OCT parameters were curvilinear, and significant correlations were noted only in eyes with severe glaucoma. The global average cpRNFL thickness showed the highest correlation with BCVA rather than TU1, TL1 sectors, or GCC parameters. Considering the wide variability of structure–visual acuity relationship in glaucoma patients, the clinicians should take other variables into account to predict the visual acuity in advanced glaucoma patients.

Keywords: visual acuity, optical coherence tomography, retinal nerve fiber layer thickness, ganglion cell complex

Glaucoma affects over 70 million people worldwide,[1,2] and is the second most frequent cause of blindness.[1] The central visual acuity is very important for glaucoma patients to enjoy their daily lives. Therefore, preservation of the visual acuity is a main concern in glaucoma treatment.

The loss of retinal ganglion cells in glaucoma can be reflected structurally as a localized or diffuse thinning of the circumpapillary retinal nerve fiber layer (cpRNFL), and its measurement has been correlated with functional damage in the visual field (VF). A number of previous studies have reported significant correlations between VF sensitivity and cpRNFL thickness in glaucoma patients using optical coherence tomography (OCT),[3–6] and scanning laser polarimetry (SLP).[6–12]

The OCT is an important method of diagnosing glaucoma and determining the progression of glaucoma.[13,14] The newer spectral domain-OCT (SD-OCT) provides much faster and more detailed structural information than previous time-domain (TD)–OCT,[15,16] and has potentially improved its ability to diagnose and observe the progression of glaucoma.[17] The RTVue-100 OCT (Optovue, Inc., Fremont, CA, USA), which is one of the commercially available SD-OCTs, includes the macular ganglion cell complex (mGCC) scan mode that measures macular inner three retinal layer thickness. Previous studies have demonstrated that ganglion cell complex (GCC) thickness measurements were significantly lower in glaucomatous eyes than in healthy eyes, and the glaucoma discrimination ability was similar to that afforded by measurement of cpRNFL thickness.[5,18–23] Because GCC scan mode is centered around the fovea and covering the central macula, GCC analysis measured by SD-OCT was demonstrated to be correlated with macular VF sensitivity.[24–26]

Although the structural and functional changes seen in glaucoma are related to the pathologic loss of retinal ganglion

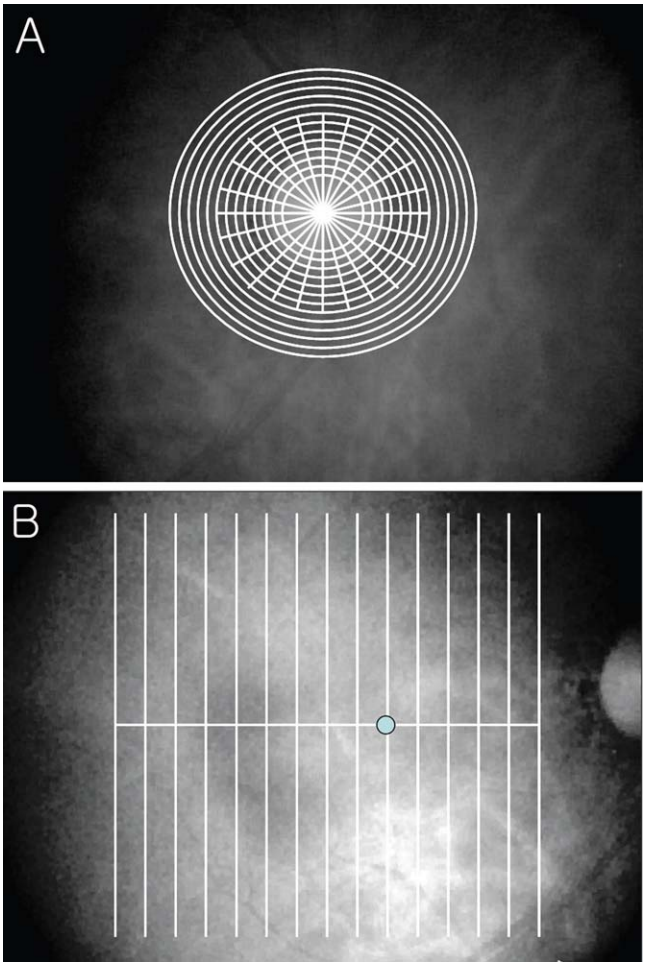

FIGURE 1. Scan patterns of RTVue SD-OCT. (**A**) The ONH scan pattern. The *white circles* and *radial lines* are the location of the B-scans that make up this scan pattern. (**B**) The GCC scan pattern superimposed on the video image. The *white lines* represent the location of the B-scans in the scan pattern. The fovea is marked with a *blue dot*.

cells (RGCs), the structure–function relationship is highly variable and imperfect. The complexity of the structure–function relationship might arise from factors, such as variability accompanying structural and functional tests, measurement scale,[27–30] spatial summation,[27–28,31,32] the lack of precise colocalization between the structural and functional measures, and interindividual physiologic variations. It has become evident that a substantial number of RGCs may need to be lost before changes are detected with standard automated perimetry (SAP). This weak relationship between structure and function in glaucoma patients using SAP as a functional test has urged alternative forms of functional test. Since the ganglion cells subserving foveal visual acuity are displaced from the fovea in the central retina, the mGCC scan might give better colocalization with foveal visual acuity than central VFs. Furthermore, retinal nerve fiber layer (RNFL) thickness measured by commercially available OCT contains more than just nerve fibers, such as non-neural or glial tissues. We hypothesized that the mGCC scan, which contains more ganglion cells by proportion, might yield stronger structure–function relationships than the cpRNFL scan.

In the present study, we assessed the relationship between various OCT parameters measured by RTVue SD-OCT and visual acuity in open-angle glaucoma (OAG) patients.

METHODS

Study Design

Participants were enrolled consecutively from the Glaucoma Clinic of Severance Hospital in Yonsei University College of Medicine from January 2010 to June 2010. The study was approved by our institutional review board and the Ethics Committee of Severance Hospital, and complied with the tenets of the Declaration of Helsinki. All patients provided written informed consent.

Patients were included if they were diagnosed with OAG, including primary OAG (POAG) and normal tension glaucoma (NTG), they had refractive errors (spherical equivalent) of $<$ +3.0 diopters (D) and $>$ −6.00 (D), and had cylinder correction within ± 3.0 (D). Patients were excluded if they had any of the following during the follow-up: development of any ocular disease, especially vitreoretinal disease or macular abnormality other than glaucoma; other diseases affecting the VFs; prior history of ocular surgery (other than uncomplicated glaucoma and cataract surgery); and significant media opacity (cataract grade $>$ N2 by lens opacities classification system [LOCS] classification). When data from both eyes were eligible for analysis, one eye from each patient was selected randomly for data analysis.

All subjects underwent Goldmann applanation tonometry, gonioscopy, and fundus examination with a +90-D lens. Automated refraction, biometry measurement, and standard VF testing were performed. The best-corrected visual acuity (BCVA) was measured with a Snellen visual acuity chart and converted to the logMAR for the statistical analyses. All eyes underwent RTVue SD-OCT after pupillary dilation (minimum diameter, 5 mm). For each patient, all examinations were performed during a single day.

Standard VF testing was performed using automated static perimetry (Humphrey Field analyzer with Swedish Interactive Thresholding Algorithm (SITA) standard 24-2 test program; Carl Zeiss Meditec, Dublin, CA, USA). The VF was considered reliable when fixation losses were less than 20%, and false-positive and false-negative errors were less than 15%. The perimeter software was used to calculate mean deviation (MD), pattern standard deviation (PSD), and VF index (VFI).

Glaucomatous eyes were defined as having glaucomatous VF defects as confirmed by at least two reliable VF examinations and presence of a compatible glaucomatous optic disc that showed increased cupping (a vertical cup-disc ratio of $>$0.7), a difference in vertical cup-disc ratio of $>$0.2 between eyes, diffuse or focal neural rim thinning, disc hemorrhage, or RNFL defects. A glaucomatous VF defect was defined as having three or more significant ($P < 0.05$) contiguous points with at least one at the $P < 0.01$ level on the same side of the horizontal meridian in the pattern deviation plot, classified as outside normal limits in the glaucoma hemifield test.[33]

Glaucoma was categorized according to the modified Hodapp-Anderson-Parrish grading scale based on the MD of VF.[34,35] Early glaucoma was defined as VF loss with an MD $\geq$ −6 dB, moderate glaucoma as an MD between −6 and −12 dB, and severe glaucoma as an MD worse than −12dB.

The cpRNFL and GCC thicknesses were measured using RTVue-100 SD-OCT (software version, 4.0.5.39), and both scan patterns of RTVue SD-OCT are shown in Figure 1.[36] All scans were performed by one experienced operator.

The cpRNFL thickness was determined by optical nerve head (ONH) mode, in which data along a 3.4-mm diameter circle around the optic disc were recalculated with a map created from en face imaging using six circular and 12 linear data inputs. Mean, superior, and inferior RNFL thicknesses

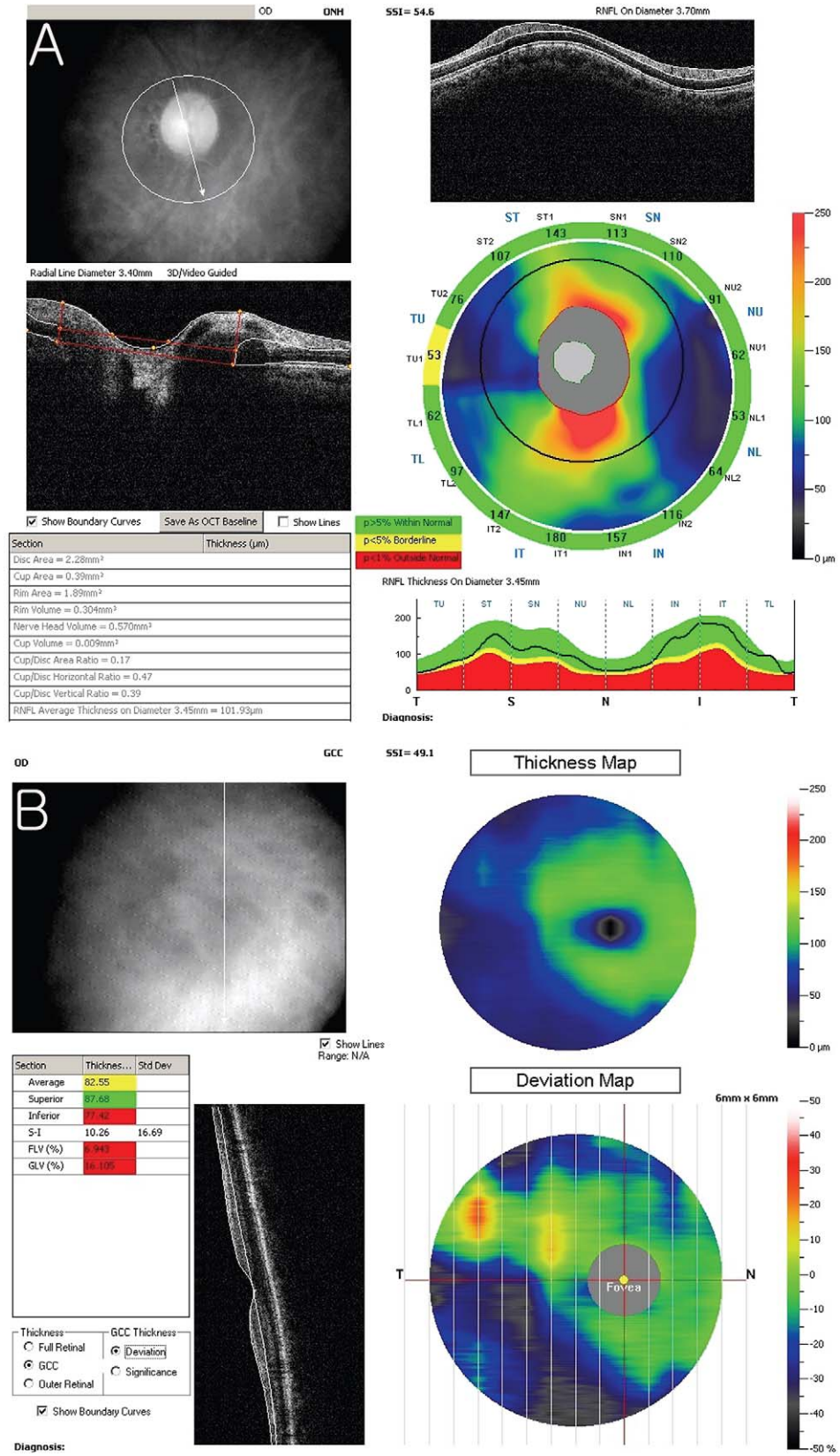

Figure 2. Map display report of RTVue SD-OCT. (**A**) The ONH report for a single eye. (**B**) The GCC report for a single eye. The GCC thickness map is at the *top* and the deviation map is *below*. The deviation map reflects the percent loss from normal, where *darker colors* represent greater loss.

Table 1. Correlation Analysis Between BCVA and Demographics, and Clinical Variables in the Subjects

	Univariate			Multivariate		
	r	β (SE)	*P* Value	*r*	β (SE)	*P* Value
Age, per y	0.120	0.001 (0.001)	0.103	0.110	0.001 (0.001)	0.157
Sex, female	0.054	0.015 (0.021)	0.465			
Central corneal thickness, per μm	−0.190	−0.001 (0.001)	0.013	−0.186	−0.001 (0.001)	0.016
Axial length, per mm	−0.001	−0.001 (0.006)	0.991			
Anterior chamber depth, per mm	0.056	0.013 (0.018)	0.466			
Spherical equivalent, per D	−0.086	−0.003 (0.003)	0.294			

P values and correlation coefficients of partial correlation analysis.

were calculated. The software also provided cpRNFL thickness values for each of the 16 individual sectors per each 22.5° rad (ST1, 0°–22.5°; ST2, 22.5°–45°; TU2, 45°–67.5°; TU1, 67.5°–90°; TL1, 90°–112.5°; TL2, 112.5°–135°; IT2, 135°–157.5°; IT1, 157.5°–180°). Map report displayed by ONH mode is shown in Figure 2A.[36]

The GCC parameters were obtained by the macular map (MM7) protocols, centered 1 mm temporal to the fovea. This protocol uses one horizontal line with a 7-mm scan length (934 A-scans), followed by 15 vertical lines with a 7-mm scan length and 0.5-mm interval (800 A-scans). The GCC thickness was measured from the internal limiting membrane to the inner plexiform layer boundary; mean, superior, and inferior GCC thicknesses were calculated. Based on the percent deviation map, two special pattern analysis parameters were provided. Global loss volume (GLV) is the integration of all negative deviation values normalized by the overall map area. Focal loss volume (FLV) is the integration of negative deviation values in the areas of significant focal loss.[19,36] Map report displayed by GCC mode is shown in Figure 2B.[36]

Image quality on the RTVue-100 OCT is determined by investigator's observation and the signal strength index (SSI) parameter. In the current study, only images with an SSI of more than 40 were used. Images also were excluded when overt misalignment of the surface detection algorithm occurred, or there was overt decentration of the measurement circle location.

Statistical Analysis

Correlation analysis between baseline characteristics (age, sex, central corneal thickness [CCT], axial length, anterior chamber depth, and spherical equivalent) and BCVA revealed that logMAR BCVA was worse for older subjects and for subjects with a thinner central cornea. (Table 1). Therefore, correlations between multiple OCT parameters and BCVA were evaluated by Pearson's partial correlation analysis after adjusting by age and CCT. We also performed the subgroup analysis after dividing the participants into two groups according to their VF severity (early-to-moderate versus advanced).

The relationships between average RNFL/GCC thickness and BCVA were evaluated with linear and nonlinear (second-order and third-order polynomial) regression analyses. The logMAR BCVA was treated as the dependent variable and average RNFL/GCC thickness as the independent variables in all regressions. Regression models were evaluated with the extra-sum-of square *F* test, which was used to test whether the alternative nonlinear model (second-order polynomial or third-order polynomial) fit the data better than the linear model.[6,37] Locally weighted scatter plot smoothing (LOWESS) curves also were used to fit the relationship graphically. The LOWESS is a modeling method that combines the linear least squares regression with the nonlinear regression.[38] Finally, receiver operating characteristic (ROC) curve analysis was performed to obtain cutoff values for multiple OCT parameters for the discrimination of eyes with decreased visual acuity. Decreased visual acuity was arbitrarily defined as a BCVA of 20/30 or less, because visual acuity of 20/30 is a cutoff value for receiving a driver's license in Korea. Statistical analysis was performed using SPSS for Windows (version 12.0.0; SPSS, Inc., Chicago, IL, USA) and the MedCalc software statistical package software version 9.6.2.0 (MedCalc Software, Mariakerke, Belgium). $P < 0.05$ was considered statistically significant.

Table 2. Characteristics of the Subjects According to the Glaucoma Severity

	Early Glaucoma, *n* = 87	Moderate Glaucoma, *n* = 39	Severe Glaucoma, *n* = 60	*P* Value*
Age, y	51.71 ± 13.25	52.25 ± 17.15	56 ± 16.48	0.224
Male sex, *n* (%)	49 (56.32)	23 (58.97)	39 (65.00)	0.571
Central cornea thickness, μm	540.57 ± 36.82	541.63 ± 32.49	529.09 ± 37.71	0.141
Axial length, mm	24.65 ± 1.51	25.20 ± 2.17	24.37 ± 1.79	0.085
Anterior chamber depth, mm	3.36 ± 0.48	3.39 ± 0.66	3.33 ± 0.68	0.892
Spherical equivalent, D	−2.15 ± 3.57	−2.72 ± 4.43	−2.37 ± 3.76	0.782
IOP, mm Hg	14.17 ± 2.98	14.07 ± 2.88	13.82 ± 4.16	0.833
Mean deviation, dB	−3.26 ± 1.49	−8.49 ± 1.94	−20.00 ± 6.09	<0.001†
Pattern SD, dB	3.57 ± 2.31	8.66 ± 3.55	11.05 ± 3.45	<0.001†
LogMAR BCVA	−0.013 ± 0.055	0.032 ± 0.068	0.147 ± 0.196	<0.001‡

The data are given as the mean ± SD.

* Value for ANOVA tests.

† Difference among severity level of glaucoma (early versus moderate, <0.001; early versus severe, <0.001; moderate versus severe, <0.001).

‡ Statistically significant difference in logMAR BCVA, which was worse in the severe glaucoma group compared to the early-to-moderate glaucoma group ($P < 0.05$, pairwise comparison after ANOVA with Bonferroni correction; early versus moderate, 0.166; early versus severe, <0.001; moderate versus severe, <0.001).

Table 3. RNFL Thickness, ONH Parameters, and GCC Parameters Obtained by RTVue SD-OCT

	Early		Moderate		Severe	
	Mean ± SD	95% CI	Mean ± SD	95% CI	Mean ± SD	95% CI
RNFL parameters						
Average, μm	94.15 ± 16.11	90.69–97.60	83.25 ± 13.54	78.86–87.64	72.80 ± 12.77	69.50–76.10
Superior hemisphere, μm	101.22 ± 19.61	97.02–105.43	88.42 ± 16.71	83.00–93.84	76.88 ± 17.37	72.39–81.37
Inferior hemisphere, μm	87.06 ± 16.10	83.61–90.51	78.09 ± 15.29	73.13–83.05	68.39 ± 11.73	65.36–71.42
ONH parameters						
Disc area, mm^2	2.51 ± 0.57	2.39–2.63	2.44 ± 0.72	2.20–2.67	2.46 ± 0.64	2.30–2.63
Rim area, mm^2	1.02 ± 0.49	0.92–1.13	0.75 ± 0.44	0.61–0.89	0.51 ± 0.50	0.38–0.64
Cup area, mm^2	1.49 ± 0.56	1.37–1.61	1.66 ± 0.66	1.45–1.88	1.95 ± 0.66	1.78–2.13
Cup-disc area ratio	0.59 ± 0.18	0.55–0.63	0.67 ± 0.17	0.61–0.73	0.79 ± 0.18	0.74–0.84
Horizontal cup-disc ratio	0.82 ± 0.16	0.79–0.86	0.86 ± 0.15	0.81–0.91	0.91 ± 0.14	0.87–0.94
Vertical cup-disc ratio	0.77 ± 0.16	0.74–0.81	0.83 ± 0.13	0.79–0.87	0.90 ± 0.14	0.86–0.93
GCC parameters						
Average, μm	84.63 ± 9.23	82.65–86.61	76.67 ± 7.51	74.24–79.10	70.51 ± 9.24	68.13–72.90
Superior, μm	87.85 ± 9.99	85.71–89.99	78.84 ± 8.63	76.04–81.64	73.08 ± 11.24	70.18–75.98
Inferior, μm	81.51 ± 10.74	79.20–83.81	75.01 ± 10.19	71.71–78.31	67.91 ± 9.66	65.42–70.41
Focal loss volume, %	5.02 ± 4.05	4.15–5.89	8.16 ± 5.00	6.54–9.78	9.06 ± 3.76	8.09–10.03
Global loss volume, %	16.70 ± 8.27	14.93–18.47	24.04 ± 7.06	21.75–26.33	29.75 ± 8.57	27.54–31.97

Results

During the enrollment period, a total of 261 eyes from 261 participants was examined. Of the eyes 45 were excluded because of poor OCT images due to low signal strength (<40 in RTVue OCT), while 30 were excluded because of improper OCT images due to scan decentration.

A total of 186 eyes of 186 patients was included in the final analysis. Glaucoma was categorized as early glaucoma ($n = 87$), moderate glaucoma ($n = 39$), or severe glaucoma ($n = 60$), according to the modified Hodapp's classification. Table 2 summarizes participants' characteristics. The mean VF MDs in the early, moderate, and severe glaucoma groups were –3.26 ± 1.49, –8.49 ± 1.94, and –20.00 ± 6.09 dB, respectively. In a pairwise comparison, the mean logMAR BCVA was significantly worse in the severe glaucoma group compared to early-to-moderate glaucoma groups, and there was no significant difference between early and moderate glaucoma group. A summary of OCT measurements of the participants are presented by disease severity in Table 3.

The correlations between OCT parameters and BCVA were examined by Pearson's partial correlation adjusted for age and central corneal thickness. (Table 4) There were significant correlations between BCVA and the overall RNFL parameters. Among all RNFL parameters, average RNFL thickness ($r = –0.447$, $P < 0.001$) showed the highest correlation with BCVA, followed by superior hemisphere ($r = –0.440$, $P < 0.001$), and the TU1 (67.5°–90°, $r = –0.427$, $P < 0.001$), TU2 (45°–67.5°, $r = –0.408$, $P < 0.001$), and TL1 (90°–112.5°, $r = –0.40$, $P < 0.001$) sectors. There also were significant correlations between BCVA and overall GCC parameters. Global loss volume ($r = 0.417$, $P < 0.001$) and average GCC thickness ($r = –0.410$, $P < 0.001$) showed the highest correlation with BCVA among GCC parameters. All ONH parameters except for disc area showed significant correlations with BCVA.

In a subgroup analysis according to glaucoma severity (early-to-moderate versus severe), the strength of the correlations between BCVA and OCT parameters differed by disease severity (Table 5). In the early-to-moderate glaucoma group, the significant correlation between the BCVA and RNFL parameters was limited only to the ST1 sector (ST1, 0°–22.5°; $r = –0.205$, $P = 0.031$). However, in the severe glaucoma

Table 4. Correlations Between RNFL Thickness and BCVA

	r	*β* (SE)	*P* Value
RNFL parameter			
Average	−0.447	0.004 (0.001)	<0.001
Superior hemisphere	−0.440	0.003 (0.001)	<0.001
Inferior hemisphere	−0.371	0.003 (0.001)	<0.001
SN1	−0.310	0.002 (0.001)	<0.001
SN2	−0.296	0.002 (0.001)	<0.001
NU2	−0.274	0.002 (0.001)	<0.001
NU1	−0.321	0.003 (0.001)	<0.001
NL1	−0.313	0.003 (0.001)	<0.001
NL2	−0.27	0.002 (0.001)	<0.001
IN2	−0.221	0.002 (0.001)	0.004
IN1	−0.248	0.002 (0.001)	0.001
IT1	−0.219	0.001 (0.001)	0.005
IT2	−0.239	0.001 (0.001)	0.002
TL2	−0.385	0.003 (0.001)	<0.001
TL1	−0.4	0.003 (0.001)	<0.001
TU1	−0.427	0.003 (0.001)	<0.001
TU2	−0.408	0.002 (0.001)	<0.001
ST2	−0.387	0.002 (0.001)	<0.001
ST1	−0.391	0.002 (0.001)	<0.001
GCC parameter			
Average	−0.410	0.005 (0.001)	<0.001
Superior GCC	−0.378	0.005 (0.001)	<0.001
Inferior GCC	−0.363	0.004 (0.001)	<0.001
Focal loss volume	0.298	0.009 (0.002)	<0.001
Global loss volume	0.417	0.006 (0.001)	<0.001
ONH parameter			
Disc area, mm2	0.008	0.002 (0.018)	0.922
Rim area, mm2	−0.383	−0.103 (0.02)	<0.001
Cup area, mm2	0.328	0.074 (0.017)	<0.001
Cup-disc area ratio	0.436	0.318 (0.052)	<0.001
Horizontal cup-disc ratio	0.276	0.268 (0.073)	<0.001
Vertical cup-disc ratio	0.299	0.28 (0.07)	<0.001

Investigative Ophthalmology & Visual Science

Table 5. Correlations Between RTVue SD-OCT Parameters and BCVA According to the Glaucoma Severity

	Early-to-Moderate			Severe		
	r	β (SE)	*P* Value*	*r*	β (SE)	*P* Value*
RNFL parameter						
Average	−0.138	−0.001 (0.001)	0.151	−0.525	0.009 (0.002)	<0.001
Superior hemisphere	−0.151	−0.001 (0.001)	0.114	−0.496	0.006 (0.001)	<0.001
Inferior hemisphere	−0.089	−0.001 (0.001)	0.352	−0.401	0.007 (0.002)	0.003
RTVueSN1	−0.116	−0.001 (0.001)	0.226	−0.321	0.003 (0.001)	0.019
RTVueSN2	−0.03	−0.001 (0.001)	0.757	−0.346	0.003 (0.001)	0.011
RTVueNU2	−0.033	−0.001 (0.001)	0.728	−0.352	0.004 (0.002)	0.01
RTVueNU1	−0.037	−0.001 (0.001)	0.701	−0.423	0.005 (0.002)	0.002
RTVueNL1	−0.084	−0.001 (0.001)	0.382	−0.42	0.006 (0.002)	0.002
RTVueNL2	−0.045	−0.001 (0.001)	0.637	−0.374	0.004 (0.002)	0.006
RTVueIN2	−0.042	−0.001 (0.001)	0.661	−0.237	0.003 (0.002)	0.088
RTVueIN1	−0.038	−0.001 (0.001)	0.690	−0.114	0.002 (0.002)	0.418
RTVueIT1	−0.072	−0.001 (0.001)	0.455	−0.042	0.001 (0.001)	0.765
RTVueIT2	−0.03	−0.001 (0.001)	0.752	−0.11	0.001 (0.001)	0.432
RTVueTL2	−0.101	−0.001 (0.001)	0.291	−0.418	0.005 (0.002)	0.002
RTVueTL1	−0.162	−0.001 (0.001)	0.091	−0.481	0.005 (0.001)	<0.001
RTVueTU1	−0.175	−0.001 (0.001)	0.066	−0.486	0.004 (0.001)	<0.001
RTVueTU2	−0.131	−0.001 (0.001)	0.171	−0.438	0.004 (0.001)	0.001
RTVueST2	−0.155	−0.001 (0.001)	0.104	−0.389	0.003 (0.001)	0.004
RTVueST1	−0.205	−0.001 (0.001)	0.031	−0.379	0.003 (0.001)	0.005
GCC parameter						
Average	−0.179	−0.001 (0.001)	0.061	−0.351	0.008 (0.003)	0.01
Superior GCC	−0.162	−0.001 (0.001)	0.088	−0.307	0.006 (0.002)	0.025
Inferior GCC	−0.140	−0.001 (0.001)	0.143	−0.308	0.007 (0.003)	0.025
Focal loss volume	0.066	0.001 (0.001)	0.493	0.273	0.015 (0.007)	0.048
Global loss volume	0.223	0.001 (0.001)	0.019	0.330	0.008 (0.003)	0.016
ONH parameter						
Disc area	0.102	0.009 (0.009)	0.288	0.055	0.019 (0.047)	0.696
Rim area	−0.156	−0.018 (0.011)	0.103	−0.391	−0.160 (0.053)	0.004
Cup area	0.220	0.021 (0.009)	0.020	0.350	0.109 (0.041)	0.011
Cup-disc area ratio	0.229	0.072 (0.03)	0.016	0.454	0.506 (0.141)	<0.001
Horizontal cup-disc ratio	0.135	0.052 (0.037)	0.160	0.361	0.517 (0.189)	0.008
Vertical cup-disc ratio	0.174	0.065 (0.035)	0.069	0.302	0.444 (0.198)	0.029

* *P* values from partial correlation analysis adjusted by age and central corneal thickness.

group, most RNFL parameters were significantly correlated with BCVA. Among all RNFL parameters, the coefficient of correlation was highest for average RNFL thickness ($r = -0.525$, $P < 0.001$), followed by superior average thickness ($r = -0.496$, $P < 0.001$), and the TU1 ($r = -0.486$, $P < 0.001$) and TL1 ($r = -0.481$, $P < 0.001$) sectors corresponding to the papillomacular bundle area. The relationship between BCVA and GCC parameters showed the similar tendencies. Although only GLV was correlated marginally with BCVA in the early-to-moderate glaucoma group, all GCC parameters were significantly correlated with BCVA in the severe glaucoma group.

The relationships between average RNFL/GCC thickness and BCVA were evaluated by regression analysis (Table 6). When logMAR BCVA was plotted against average RNFL/GCC thickness, second-order polynomial models fit better than the linear model. The structure–function relationship was better explained with nonlinear models when BCVA was plotted against average RNFL thickness ($P < 0.001$). Nonlinear models also better explained the relationship between BCVA and average GCC thickness ($P = 0.002$). Figure 3 shows the structure–function relationship between the average RNFL/GCC thickness and logMAR BCVA, each line of the graph indicating linear, quadratic regression and LOWESS fit.

After defining decreased BCVA arbitrarily as a Snellen BCVA of 20/30 or less, the area under the ROC (AUROC) curve analysis was performed to assess the ability of variable OCT parameters to detect decreased BCVA. Table 7 shows the ROC curve areas with 95% confidence intervals (CIs). The AUROCs of the average RNFL thickness and average GCC thickness were 0.910 (95% CI, 0.856–0.965) and 0.874 (95% CI, 0.795–0.953), respectively. Among variable OCT parameters, the TL1 sector had the highest AUROC at 0.924 (95% CI, 0.867–0.981),

Table 6. Regression Analysis Between Average RNFL/GCC Thickness and BCVA

	Linear				Second Order Quadratic				Third Order Cubic				Linear vs. Second	Linear vs. Third	Second vs. Third
	R^2	RMSE	*F*	*P*	R^2	RMSE	*F*	*P*	R^2	RMSE	*F*	*P*	*P*	*P*	*P*
RNFL average	0.236	0.128	16.87	<0.001	0.306	0.122	17.93	<0.001	0.306	0.122	14.26	<0.001	<0.001	<0.001	0.888
GCC average	0.205	0.13	14.11	<0.001	0.252	0.127	13.76	<0.001	0.256	0.127	11.14	<0.001	0.002	0.006	0.397

RMSE, root mean square error.

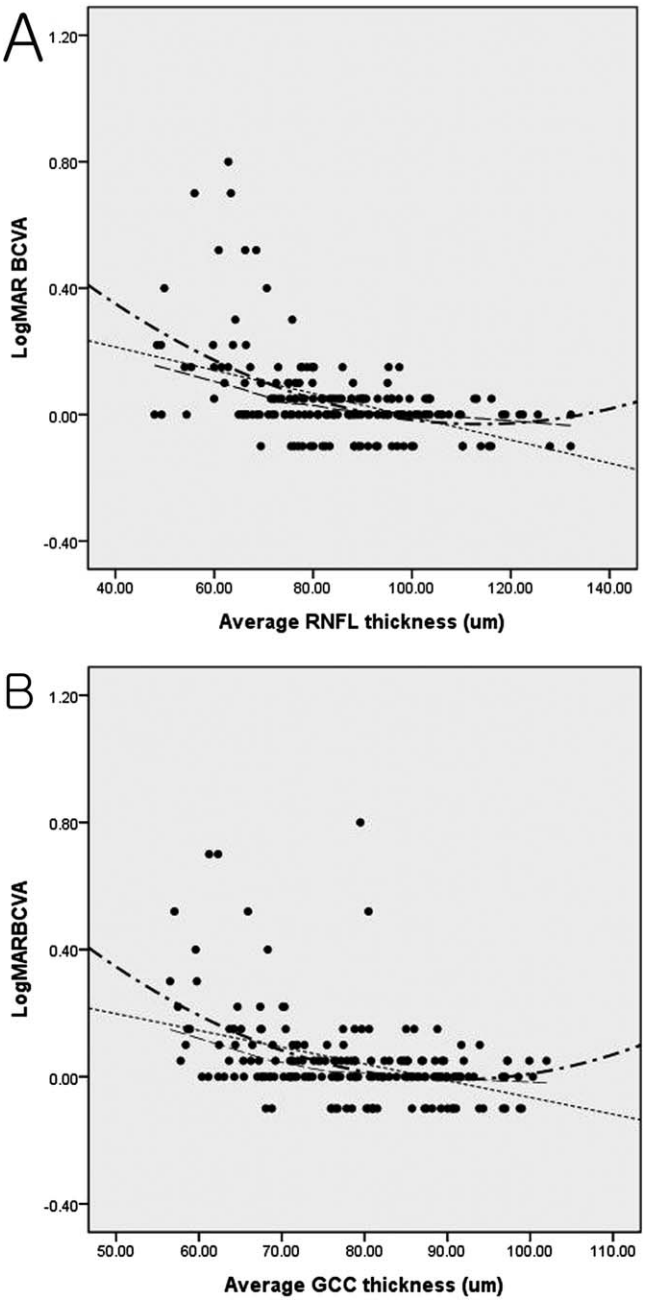

FIGURE 3. Scatter plots showing the correlation between the logMAR BCVA and average cpRNFL/mGCC thickness measured by RTVue SD-OCT. (**A**) Average cpRNFL thickness versus logMAR BCVA. (**B**) Average mGCC thickness versus logMAR BCVA (- - - - - - - -, — · — · —, — — — —, each *line* indicates that linear regression, quadratic regression, and LOWESS fit).

although there were no statistically significant differences in the ROC curve areas for these parameters ($P > 0.05$ for all comparisons). The cutoff values for average RNFL thickness, average GCC thickness, and TL1 sector for eyes with a BCVA of $< 20/30$ were 70.5, 70.3, and 51.5 μm, respectively.

DISCUSSION

Our study demonstrated that the relationship between logMAR BCVA and SD-OCT parameters in OAG patients was curvilinear, and significant correlations were noted only in eyes with severe disease status. Although sectoral analysis of the different regions of cpRNFL thickness showed that RNFL sectors corresponding to the papillomacular bundle area had the highest correlation with the BCVA, the global average cpRNFL thickness showed the highest correlation with BCVA rather than cpRNFL thickness at TU1, TL1 sectors, or GCC parameters. To our knowledge, this is the first study exploring the relationship between visual acuity and structural parameters measured by SD-OCT in glaucoma patients.

Glaucoma generally is known to be a disease in which central visual acuity is relatively well-preserved until the late stages of the disease. Although visual acuity is a major concern for glaucoma patients, there has been limited data regarding visual acuity in glaucoma patients, because visual acuity is affected by numerous factors other than glaucoma. Especially glaucoma and cataracts are frequent causes of decreased visual acuity among the elderly, and these conditions often coexist.[39] To exclude the possibility that visual acuity is being decreased by other factors, we have applied strict criteria for patient selection. We included glaucoma patients without any other ocular diseases, especially vitreoretinal disease or macular abnormality, and excluded patients with cataract grade $>$ N2 by LOCS classification.

In our study, we observed that the reduction of BCVA in glaucoma patients occurred in advanced disease state. In early-to-moderate glaucoma, no patient had decreased visual acuity (BCVA of 20/30 or less). On the other hand, 25% (15/60) of advanced glaucoma patients had decreased visual acuity. This finding is consistent with previous studies in that superotemporal and inferotemporal sectors are the most commonly affected areas in glaucoma, and that RNFL thickness in the papillomacular bundle area usually is preserved until the late stage of glaucoma.

We found that significant correlations between BCVA and multiple SD-OCT parameters were limited only in advanced glaucoma patients. Structure–function relationships in glaucomatous eyes tend to be more significant in advanced stage,[6] because the strength of relationship always increases with the range of disease, and the range of disease actually is much greater in the "severe" band.

In plotting visual acuity against average RNFL/GCC thickness, second-order polynomial models better described the relationships when compared to linear models. The finding that nonlinear models better describe the structure–function relationship is understandable given that we are plotting a logarithmic measure (logMAR BCVA) against a linear measure (structural measures). Our results confirmed that VF changes are less apparent in the early stage of structural damage, and as the glaucoma damage becomes severe, structural parameters, such as cpRNFL thickness, reach a base level beyond which only VF declines. Previous studies reported that the relationship between decibel differential light sensitivity (DLS) and ganglion cell number is curvilinear,[40–42] and the investigators attributed it to the fact that the curvilinear relationship may be explained at least in part by the logarithmic scale. Garway-Heath et al.[29] reported that there is a curvilinear relationship between dB DLS and pattern electroretinogram (PERG) amplitude and neuroretinal rim area, and a linear relationship between 1/Lambert DLS and those parameters. They concluded that there is a continuous structure–function relationship, and that the impression of a functional reserve results from the logarithmic (dB) scaling of the VF. More recently, Redmond et al.[43] investigated the relationship between peripheral grating resolution acuity (PGRA) and RNFL thickness measured by OCT in healthy subjects and patients with early glaucoma. That study demonstrated that structure/function relationships are not significantly nonlinear, when measurements are expressed on a log-log scale.

Investigative Ophthalmology & Visual Science

Table 7. The AUROC Values Obtained for Multiple SD-OCT Parameters as Predictors of Decreased Visual Acuity — Final BCVA of 20/30 or Less

OCT Parameter	AUROC	SE	*P* Value	Cutoff Value	Sensitivity, %	Specificity, %
RNFL parameters						
Average	0.910	0.028	0.000	70.52	86.9	92.3
Superior hemisphere	0.886	0.038	0.000	70.08	88.8	84.6
Inferior hemisphere	0.884	0.028	0.000	70.42	73.8	100
SN1	0.801	0.043	0.000	90.00	68.1	100
SN2	0.789	0.054	0.000	87.50	72.5	92.3
NU2	0.772	0.058	0.000	71.50	65.6	92.3
NU1	0.839	0.042	0.000	53.50	71.3	92.3
NL1	0.751	0.064	0.000	46.50	84.4	69.2
NL2	0.730	0.060	0.001	56.50	81.3	61.5
IN2	0.729	0.055	0.001	91.50	55.5	84.6
IN1	0.768	0.044	0.000	95.50	52.5	92.3
IT1	0.724	0.055	0.002	89.00	52.5	84.6
IT2	0.766	0.049	0.000	70.50	72.5	76.9
TL2	0.921	0.024	0.000	57.50	75.0	100
TL1	0.924	0.029	0.000	51.50	73.8	92.3
TU1	0.906	0.030	0.000	53.50	78.1	92.3
TU2	0.863	0.039	0.000	63.50	81.3	92.3
ST2	0.822	0.040	0.000	105.50	63.1	92.3
ST1	0.814	0.051	0.000	98.50	75.60	84.60
GCC parameters						
Average	0.874	0.040	0.000	70.3	79.4	84.6
Superior	0.845	0.053	0.000	70.3	83.1	84.6
Inferior	0.847	0.040	0.000	66.3	76.9	84.6
FLV	0.796	0.046	0.000	9.75	76.9	77.5
GLV	0.821	0.057	0.000	28.83	76.9	77.5
ONH parameters						
Disc area	0.522	0.087	0.765	3.42	41.7	92.5
Rim area	0.842	0.055	0.000	0.39	81.8	83.3
Cup area	0.732	0.063	0.002	1.77	91.7	60.4
CDR	0.836	0.059	0.000	0.85	83.3	83.6
HCDR	0.785	0.061	0.000	0.96	83.3	74.8
VCDR	0.779	0.057	0.000	0.88	91.7	66.0

Certainly, the logarithmic scaling is not the only reason for a curvilinear relationship in the current study. According to the previous studies, which investigated the topography of ganglion cells in human retina and psychophysical localization of the human visual streak,[44–46] foveal resolution acuity is limited optically for visual stimulus in that spatial frequencies higher that the resolution limit of the retina do not get through the optics of the eye. So, the optics of the eye, not the ganglion cell receptive field spacing, might limit visual acuity until a lot of RGCs have gone. This might be one of the reasons for the curvilinear structure/function relationship in the current study.

Our results also demonstrated that visual acuity can be highly variable, even if patients have the same RNFL or GCC thickness. For example if average RNFL thickness is approximately 70 μm, then BCVA can range from better than 20/20 to 20/100 or worse. This variability has been reported in many studies correlating structure–function relationship in glaucoma patients. As various factors, including optical factors, can influence the central visual acuity, it is not possible to estimate central visual acuity from RNFL thickness or ganglion cell thickness measured by OCT alone. Further study is needed to evaluate the structure–visual acuity relationship considering those factors.

One of the most interesting points in this study was the result of sectoral analysis. The investigators expected RNFL thickness at the papillomacular bundle area and GCC parameters might have a better correlation with BCVA in glaucoma patients, because those parameters may be more effective to predict central involvement of VF. As expected, TL1 and TU1 sectors corresponding to the papillomacular bundle area showed the highest correlation among 16 RNFL sectors. However, among all SD-OCT parameters, the global average RNFL thickness revealed the highest correlation with the BCVA and GCC parameters were not superior to average RNFL thickness in predicting decreased BCVA. It usually is reported that the best way to evaluate the structure–function association in glaucoma is to compare local sensitivity to local structural measurement, maximizing the colocalization of the two measurements. The reason for disparity between our results and expectation might be explained by the difference in the range of multiple RTVue SD-OCT parameters, and the average measure generally is less noisy than any of the regions. Sectoral analysis actually leads to worse colocalization in that the fibers in a particular sector do not represent the functional region in question (the fovea), but a large arcuate section of the retina. Furthermore, the decrease in temporal cpRNFL thickness might not reflect a loss of RGC accurately because the temporal cpRNFL thickness generally is thinner than the superior or inferior cpRNFL and there exist anatomic variations, such as peripapillary atrophy, that can cause larger measurement errors in the temporal cpRNFL. We also speculated that artificial segmentation provided by RTVue SD-OCT (macular GCC scan or ONH scan) is different from real anatomic boundary determining visual acuity. Additional research is needed to answer this question.

A recent study by Na et al.[25] investigated that GCC thickness determined by RTVue SD-OCT showed a statistically

significant structure–function association with macular VF and the strength of the association was greater than that of the macular cpRNFL thickness with macular VF in some areas. Another study by Shin et al.[24] reported that macular ganglion cell–inner plexiform layer (GCIPL) thickness values may provide more valuable information than temporal cpRNFL thickness values for understanding the structure–function relationships of the macular region in glaucoma patients. Our study is different from those studies in that we used logMAR BCVA as a functional outcome, in contrast those studies used more subdivided VF data. Visual acuity, as a functional outcome in the current study, might be more integrated and gross function compared to subdivided VF data. As we used transformed logMAR BCVA, this might not reflect the subtle change of function in glaucoma patients. Omodaka et al.[47] recently explored the relationship between BCVA and RNFL thickness using Stratus OCT, and found that the mid temporal (mT) sector representing the papillomacular bundle showed the highest correlation with BCVA. They suggested 39 μm of mT sector as a cut off value for decreased visual acuity (<20/20), which is lower than ours. This may be due to the fact that RNFL thickness measured by RTVue OCT has higher values than those by Stratus OCT,[48] and the profile of the study population was different.

We also calculated a cutoff value for the prediction of decreased visual acuity, defined as a Snellen BCVA of 20/30 or less. The RNFL parameters, including average thickness and RNFL sectors corresponding to the papillomacular area (TL1, TL2, TU1) ,showed the largest AUROC values among multiple OCT parameters, although no statistically significant difference was noted. These values may be useful in clinical practice.

There were several limitations in this study. The present study included glaucoma patients, not representing the full spectrum of glaucomatous damage, including suspected cases of glaucoma. The patients who were classified in the glaucoma suspect group might be too diverse, from patients who have a normal structure and function except a high IOP to patients who have a very early glaucomatous abnormality that is not yet reflected within the available diagnostic tests. This spectral diversity might inevitably weaken the structure–function relationship, we did not include a glaucoma suspect group in the present study. As we did not analyze the VF data of the subjects, further study is needed to evaluate the relationship between VF data and visual acuity. It is well known that VF examination using central 10-2 program provides more valuable information in the patients with central VF defect; correlation between visual acuity and subdivided VF data would give us a valuable information. We used the transformed logMAR BCVA derived from the Snellen chart, rather than the logMAR Early Treatment of Diabetes Retinopathy Study (ETDRS) chart, which is the gold standard for acuity measurement in research. The scale of the Snellen chart is not truly interval in nature and different numbers of letters on each line may lead to different legibility due to crowding effects. Considering that Snellen and logMAR charts have been shown to give very different acuity measurements, this transformed logMAR scale might not reflect the subtle change of visual acuity especially at the upper end (lower acuity). Furthermore, the RTVue OCT cannot offer more sectoral analysis of perimacular GCC, and we just analyzed limited data of GCC (average, superior, and inferior GCC thickness). If subdivided perimacular GCC data had been available, the results would be more meaningful.

In spite of these limitations, the current study is exploratory in nature and is the first study tokn evaluating the structure–function relationship, treating central visual acuity as a main functional outcome, and combining it with multiple structural parameters measured by RTVue SD-OCT.

In conclusion, the relationship between central visual acuity and RTVue SD-OCT parameters in OAG patients was curvilinear, and significant correlations were noted only in severe glaucoma patients. Of all RTVue SD-OCT parameters, the global average cpRNFL thickness showed the highest correlation with BCVA rather than cpRNFL thickness at TU1, TL1 sectors or GCC parameters. Considering the wide variability of the structure–visual acuity relationship in glaucoma patients in the current study, it is not possible to estimate central visual acuity from SD-OCT data alone. Therefore, clinicians should take other clinical and demographic factors into account to predict the visual acuity in glaucoma patients when the disease progresses to the advanced stage.

Acknowledgments

Presented as a poster at annual meeting of the Association for Research in Vision and Ophthamology, Fort Lauderdale, Florida, United States, May 1–5, 2011.

Supported by a grant of the Korea Health technology R&D project; Ministry of Health Welfare, Republic of Korea (A101727). The authors alone are responsible for the content and writing of the paper.

Disclosure: **J.H. Kim**, None; **H.S. Lee**, None; **N.R. Kim**, None; **G.J. Seong**, None; **C.Y. Kim**, None

References

1. Quigley HA. Number of people with glaucoma worldwide. *Br J Ophthalmol*. 1996;80:389–393.
2. Resnikoff S, Pascolini D, Etya'ale D, et al. Global data on visual impairment in the year 2002. *Bull World Health Organ*. 2004; 82:844–851.
3. Ajtony C, Balla Z, Somoskeoy S, Kovacs B. Relationship between visual field sensitivity and retinal nerve fiber layer thickness as measured by optical coherence tomography. *Invest Ophthalmol Vis Sci*. 2007;48:258–263.
4. Wollstein G, Schuman JS, Price LL, et al. Optical coherence tomography (OCT) macular and peripapillary retinal nerve fiber layer measurements and automated visual fields. *Am J Ophthalmol*. 2004;138:218–225.
5. Kim NR, Lee ES, Seong GJ, Kim JH, An HG, Kim CY. Structure–function relationship and diagnostic value of macular ganglion cell complex measurement using Fourier-domain OCT in glaucoma. *Invest Ophthalmol Vis Sci*. 2010;51:4646–4651.
6. Leung CK, Chong KK, Chan WM, et al. Comparative study of retinal nerve fiber layer measurement by Stratus OCT and GDx VCC, II: structure/function regression analysis in glaucoma. *Invest Ophthalmol Vis Sci*. 2005;46:3702–3711.
7. Choi J, Kim KH, Lee CH, et al. Relationship between retinal nerve fibre layer measurements and retinal sensitivity by scanning laser polarimetry with variable and enhanced corneal compensation. *Br J Ophthalmol*. 2008;92:906–911.
8. Schlottmann PG, De Cilla S, Greenfield DS, Caprioli J, Garway-Heath DF. Relationship between visual field sensitivity and retinal nerve fiber layer thickness as measured by scanning laser polarimetry. *Invest Ophthalmol Vis Sci*. 2004;45:1823–1829.
9. Mai TA, Reus NJ, Lemij HG. Structure–function relationship is stronger with enhanced corneal compensation than with variable corneal compensation in scanning laser polarimetry. *Invest Ophthalmol Vis Sci*. 2007;48:1651–1658.
10. Bowd C, Zangwill LM, Weinreb RN. Association between scanning laser polarimetry measurements using variable corneal polarization compensation and visual field sensitivity in glaucomatous eyes. *Arch Ophthalmol*. 2003;121:961–966.

11. Reus NJ, Lemij HG. The relationship between standard automated perimetry and GDx VCC measurements. *Invest Ophthalmol Vis Sci*. 2004;45:840–845.
12. Leung CK, Medeiros FA, Zangwill LM, et al. American Chinese glaucoma imaging study: a comparison of the optic disc and retinal nerve fiber layer in detecting glaucomatous damage. *Invest Ophthalmol Vis Sci*. 2007;48:2644–2652.
13. Huang ML, Chen HY. Development and comparison of automated classifiers for glaucoma diagnosis using Stratus optical coherence tomography. *Invest Ophthalmol Vis Sci*. 2005;46:4121–4129.
14. Parikh RS, Parikh S, Sekhar GC, et al. Diagnostic capability of optical coherence tomography (Stratus OCT 3) in early glaucoma. *Ophthalmology*. 2007;114:2238–2243.
15. Wojtkowski M, Bajraszewski T, Gorczyn' ska I, et al. Ophthalmic imaging by spectral optical coherence tomography. *Am J Ophthalmol*. 2004;138:412–419.
16. Chen TC, Cense B, Pierce MC, et al. Spectral domain optical coherence tomography: ultra-high speed, ultra-high resolution ophthalmic imaging. *Arch Ophthalmol*. 2005;123:1715–1720.
17. Kim NR, Lee ES, Seong GJ, Choi EH, Hong S, Kim CY. Spectral-domain optical coherence tomography for detection of localized retinal nerve fiber layer defects in patients with open-angle glaucoma. *Arch Ophthalmol*. 2010;128:1121–1128.
18. Seong M, Sung KR, Choi EH, et al. Macular and peripapillary retinal nerve fiber layer measurements by spectral domain optical coherence tomography in normal-tension glaucoma. *Invest Ophthalmol Vis Sci*. 2010;51:1446–1452.
19. Tan O, Chopra V, Lu AT, et al. Detection of macular ganglion cell loss in glaucoma by Fourier-domain optical coherence tomography. *Ophthalmology*. 2009;116:2305–2314.
20. Rao HL, Zangwill LM, Weinreb RN, Sample PA, Alencar LM, Medeiros FA. Comparison of different spectral domain optical coherence tomography scanning areas for glaucoma diagnosis. *Ophthalmology*. 2010;117:1692–1699.
21. Nakatani Y, Higashide T, Ohkubo S, Takeda H, Sugiyama K. Evaluation of macular thickness and peripapillary retinal nerve fiber layer thickness for detection of early glaucoma using spectral domain optical coherence tomography. *J Glaucoma*. 2011;20:252–259.
22. Huang JY, Pekmezci M, Mesiwala N, Kao A, Lin S. Diagnostic power of optic disc morphology, peripapillary retinal nerve fiber layer thickness, and macular inner retinal layer thickness in glaucoma diagnosis with fourier-domain optical coherence tomography. *J Glaucoma*. 2011;20:87–94.
23. Garas A, Vargha P, Hollo G. Diagnostic accuracy of nerve fibre layer, macular thickness and optic disc measurements made with the RTVue-100 optical coherence tomography to detect glaucoma. *Eye (Lond)*. 2011;25:57–65.
24. Shin HY, Park HY, Jung KI, Park CK. Comparative study of macular ganglion cell-inner plexiform layer and peripapillary retinal nerve fiber layer measurement: structure–function analysis. *Invest Ophthalmol Vis Sci*. 2013;54:7344–7353.
25. Na JH, Kook MS, Lee Y, Baek S. Structure–function relationship of the macular visual field sensitivity and the ganglion cell complex thickness in glaucoma. *Invest Ophthalmol Vis Sci*. 2012;53:5044–5051.
26. Sato S, Hirooka K, Baba T, Tenkumo K, Nitta E, Shiraga F. Correlation between the ganglion cell-inner plexiform layer thickness measured with cirrus HD-OCT and macular visual field sensitivity measured with microperimetry. *Invest Ophthalmol Vis Sci*. 2013;54:3046–3051.
27. Garway-Heath DF, Caprioli J, Fitzke FW, Hitchings RA. Scaling the hill of vision: the physiological relationship between light sensitivity and ganglion cell numbers. *Invest Ophthalmol Vis Sci*. 2000;41:1774–1782.
28. Swanson WH, Felius J, Pan F. Perimetric defects and ganglion cell damage: interpreting linear relations using a two-stage neural model. *Invest Ophthalmol Vis Sci*. 2004;45:466–472.
29. Garway-Heath DF, Holder GE, Fitzke FW, Hitchings RA. Relationship between electrophysiological, psychophysical, and anatomical measurements in glaucoma. *Invest Ophthalmol Vis Sci*. 2002;43:2213–2220.
30. Malik R, Swanson WH, Garway-Heath DF. Development and evaluation of a linear staircase strategy for the measurement of perimetric sensitivity. *Vision Res*. 2006;46:2956–2967.
31. Anderson RS. The psychophysics of glaucoma: improving the structure/function relationship. *Prog Retin Eye Res*. 2006;25:79–97.
32. Pan F, Swanson WH. A cortical pooling model of spatial summation for perimetric stimuli. *J Vis*. 2006;6:1159–1171.
33. Anderson DR. *Automated Static Perimetry*, 2nd ed. St. Louis, MO: Mosby; 1999:10–35.
34. Hodapp E, Parrish RK, Anderson DR. *Clinical Decisions in Glaucoma*. St Louis, MO: Mosby; 1993:52–61.
35. Budenz DL, Rhee P, Feuer WJ, McSoley J, Johnson CA, Anderson DR. Comparison of glaucomatous visual field defects using standard full threshold and Swedish interactive threshold algorithms. *Arch Ophthalmol*. 2002;120:1136–1141.
36. Weinreb RN, Varma R, Araie M, et al. *RTVue Fourier-Domain Optical Coherence Tomography Primer Series: Vol. III Glaucoma*. Fremont, CA: Optovue, Inc.; 2010.
37. Burnham KP, Anderson DR. Information and likelihood theory: a basis for model selection and inference. In: *Model Selection and Multimodel Inference: A Practical Information and Theoretic Approach*. New York, NY: Springer; 2002:49–97.
38. Cleveland WS, Devlin SJ. Locally weighted regression: an approach to regression analysis by local fitting. *J Am Stat Assoc*. 1988;83:596–610.
39. Quillen DA. Common causes of vision loss in elderly patients. *Am Fam Physician*. 1999;60:99–108.
40. Quigley HA, Dunkelberger GR, Green WR. Retinal ganglion cell atrophy correlated with automated perimetry in human eyes with glaucoma. *Am J Ophthalmol*. 1989;107:453–464.
41. Kerrigan-Baumrind LA, Quigley HA, Pease ME, Kerrigan DF, Mitchell RS. Number of ganglion cells in glaucoma eyes compared with threshold visual field tests in the same persons. *Invest Ophthalmol Vis Sci*. 2000;41:741–748.
42. Harwerth RS, Carter-Dawson L, Shen F, Smith EL III, Crawford ML. Ganglion cell losses underlying visual field defects from experimental glaucoma. *Invest Ophthalmol Vis Sci*. 1999;40:2242–2252.
43. Redmond T, Anderson RS, Russell RA, Garway-Heath DF. Relating retinal nerve fiber layer thickness and functional estimates of ganglion cell sampling density in healthy eyes and in early glaucoma. *Invest Ophthalmol Vis Sci*. 2013;54:2153–2162.
44. Curcio CA, Allen KA. Tomography of ganglion cells in human retina. *J Comp Neurol*. 1990;300:5–25.
45. Anderson RS, Wilkinson MO, Thibos LN. Psychophysical localization of the human visual streak. *Optom Vis Sci*. 1992;69:171–174.
46. Anderson RS, Ennis FA. Foveal and peripheral thresholds for detection and resolution of vanishing optotype tumbling E's. *Vision Res*. 1999;39:4141–4144.
47. Omodaka K, Nakazawa T, Yokoyama Y, Doi H, Fuse N, Nishida K. Correlation between peripapillary macular fiber layer thickness and visual acuity in patients with open-angle glaucoma. *Clin Ophthalmol*. 2010;21:629–635.
48. Lee ES, Kang SY, Choi EH, et al. Comparisons of nerve fiber layer thickness measurements between Stratus, Cirrus, and RTVue OCTs in healthy and glaucomatous eyes. *Optom Vis Sci*. 2011;88:751–758.

Investigative Ophthalmology & Visual Science